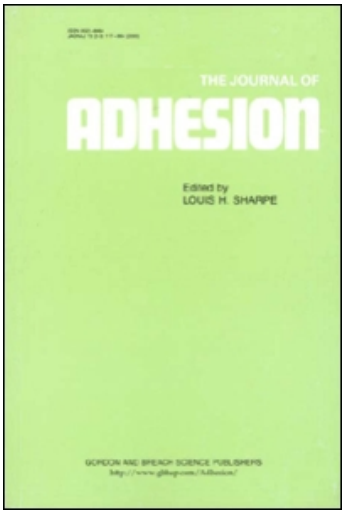

The Journal of Adhesion
Publication details, including instructions for authors and subscription information:
http://www.informaworld.com/smpp/title~content=t713453635

Effect of High Modulus Polyethylene Fibre Surface Treatment on Epoxy Resin Composite Impact Properties

D. W. Woods[a]; P. J. Hine[a]; R. A. Duckett[a]; I. M. Ward[a]
[a] IRC in Polymer Science and Technology, University of Leeds, Leeds, UK

To cite this Article Woods, D. W. , Hine, P. J. , Duckett, R. A. and Ward, I. M.(1994) 'Effect of High Modulus Polyethylene Fibre Surface Treatment on Epoxy Resin Composite Impact Properties', The Journal of Adhesion, 45: 1, 173 — 189
To link to this Article: DOI: 10.1080/00218469408026637
URL: http://dx.doi.org/10.1080/00218469408026637

J. Adhesion, 1994, Vol. 45, pp. 173–189
Reprints available directly from the publisher
Photocopying permitted by license only

Printed in the United States of America

Effect of High Modulus Polyethylene Fibre Surface Treatment on Epoxy Resin Composite Impact Properties*

D. W. WOODS,** P. J. HINE, R. A. DUCKETT and I. M. WARD

IRC in Polymer Science and Technology, University of Leeds, Leeds, LS2 9JT, UK

(Received February 27, 1993; in final form June 4, 1993)

Unidirectional and cross-ply epoxy resin composites have been made using both untreated and plasma treated melt-spun and gel-spun high-modulus polyethylene fibres. Interlaminar shear strength adhesion measurements have been related to high speed flexural strength and impact energy absorption.

KEY WORDS epoxy resin composites; high-modulus polyethylene fibre; fibers; impact; plasma treatment; high-speed three-point bend test; interlaminar shear strength (ILSS); clamped plate impact test; falling weight test.

INTRODUCTION

High modulus polyethylene (HMPE) fibres are characterised by high strength, high modulus, high breaking elongation and low density. The use of these fibres in composite structures, particularly in combination with brittle high modulus fibres such as glass or carbon, enables a strong and tough energy absorbent composite to be produced.[1,2] Mechanical failure of a fibre/resin composite is a very complex process, being dependent on the test mode, the fibre and the resin properties and the manner in which they are combined in the laminate.[3]

One of the more important parameters of a composite is the impact performance. This is frequently measured in terms of impact resistance, where the frequency of projectile penetration is determined from a V_{50} test. More detailed data can be obtained from impact absorption measurements using an instrumented falling weight test.[4] This technique has been used by a number of workers to examine the relation between fibre/resin adhesion and impact properties. For example, it has been shown that the V_{50} impact performance of epoxy resin polyethylene/carbon hybrid composites containing high modulus fabric is reduced after the adhesion between the fabric and the resin is increased by chromic acid treatment.[5] A similar

*Presented at the International Symposium on "The Interphase" at the Sixteenth Annual Meeting of The Adhesion Society, Inc., Williamsburg, Virginia, U.S.A., February 21–26, 1993.
**Corresponding author.

increase in adhesion and reduction in V_{50} performance has been obtained for aramid fabric composites after ammonia plasma treatment of the aramid fabric[6] and also for gel-spun high-modulus polyethylene fabric composites after ammonia plasma treatment of the polyethylene fabric.[7] More limited data are available for oxygen-plasma-treated polyethylene fabric composites, which show the low speed flexural strength increasing after ammonia plasma treatment.[8]

This work provides further results for high-modulus polyethylene fibre using oxygen-plasma treatment to produce a range of adhesion from three fibre types. Particular features of this work are the composite construction in which the parallel array of fibres are stacked alternately at right angles using a prepreg method, the use of unidirectional composites for shear failure testing at high speed, and the high-speed flexural impact test carried out at a speed comparable with that of the falling weight impact test.

The plasma treatment process used here was originally developed as a batch process.[1] This has now been developed further as a continuous process to provide the larger quantities of fibre required for making 0/90 composites.

The failure mode of the composite also depends on the test used. This work is an attempt to identify and understand the effects of HMPE fibre surface treatment, HMPE fibre properties and test mode on the impact performance of HMPE composites in terms of energy absorption and interlaminar shear strength.

In a recent investigation in this laboratory,[9] a comparative study of the impact behaviour of 0/90 cross-ply HMPE fibre/epoxy resin composites was undertaken using the falling weight impact test. Both melt- and gel-spun fibres were used, and the tests were carried out with both untreated and plasma-treated fibres. Similar falling weight tests have been carried out using the present composites in order to make direct comparison with a new custom-built, high-speed, three-point bend test and with the previous study which also used the falling weight impact test.

EXPERIMENTAL

Composite Construction

The properties of the HMPE fibres used in this study are listed in Table I (Tenfor, melt spun; Spectra and Dyneema, gel spun).

Composites containing approximately 54 Vol% of high modulus polyethylene fibre in an epoxy resin matrix were made using a prepreg method in which the composite is formed with adjacent fibre layers at right angles. The prepregs were prepared using a 42 gm^{-2}, partially-cured epoxy resin film (Ciba-Geigy, Type 913) cast on a 0.5 m wide release paper. The resin-coated release paper was mounted on a 1.3 m diameter drum which was rotated at 4 rpm. The fibre was wound on the drum by traversing a fibre feed guide across the drum surface at a constant speed of 5 mm/min to give the required final composite fibre volume fraction of 54%. A second resin film on release paper was then applied over the wound fibre and the prepreg then compacted manually at a temperature below 100°C using a heated iron. The prepreg assembly was then cut to the required size of 250×250 mm and

TABLE I
HMPE Fibre properties

Fibre*	Fibre denier g/9km	Number of filaments	Filament diameter mm	Breaking strength GPa	Initial modulus GPa	Molecular weight Mw
Tenfor	1800	1580	0.013	1.3	60	130,000
Spectra	665	130	0.027	2.6	120	1,500,000
Dyneema	395	390	0.012	2.5	90	1,300,000

*Tenfor is made by Snia Fibre Ltd, Milan, Italy
Spectra is made by Allied Signal, USA
Dyneema is made by D.S.M., Holland

consolidated in a press at room temperature. The release paper was removed from each of the 24 prepreg layers which were then laid in a 0/90 configuration to form the composite. The completed composite was then heated and cured under a pressure of 5 bars (0.5 MPa) in a press for 3 hours at 100°C to produce a 250 × 250 mm composite having a total thickness of approximately 3.5 mm and a layer thickness of approximately 0.15 mm.

Plasma Treatment of Fibre

The surfaces of the HMPE fibres were modified using a continuous plasma treatment process developed for HMPE fibres which produces surface oxidation, surface cross linking and etching of the filament surface.[10,11,12] The use of gas plasma for modifying the surface of HMPE fibres to improve adhesion is a proprietary process which is covered by patents in North America and Europe.[13]

In the continuous plasma treatment process, the fibre passes through an evacuated small diameter glass reactor tube 2 metres in length which is supplied with oxygen at a flow rate of 17 cc min^{-1} to give a gas pressure of 0.4 torr. Two electrodes are mounted outside the tubes and are supplied with radio frequency power (13.56 MHz) to energise the oxygen in the cylinder and form the gas plasma. A range of highly-active species such as ions and free electrons are produced by the RF-excited oxygen, all of which produce changes in the fibre surface characteristics. By careful adjustment of the fibre entrance and exit zones, using narrow bore tubes, the fibre is successfully transferred from the supply package at ambient pressure to the treatment zone at low pressure and then to the wind up package at ambient pressure. The fibres were treated at a speed of 40 m/min with a corresponding treatment time of 3 s at 300 watts power input.

Testing

Impact tests were carried out using a custom-built, servo hydraulic three-point bend tester made by RDP Howden Ltd and also a falling weight clamped plate impact tester made by Rosand (UK) Ltd. A particular feature of the three-point bend tester is the facility to arrest the impactor at any point of the test. The sample can then be inspected and any sample damage related to the corresponding load/deflection curve.

The three-point bend test used an $80 \times 10 \times 3.5$ mm sample and a testing span of 60 mm in accordance with the recommendations of the ASTM standard test method D790-80, at a testing speed of 1 ms^{-1}. A total deflection of 20 mm was applied at the centre of the specimen, corresponding to a maximum surface strain of 10%, and the sample inspected for damage after the test. The resultant bending load curve was displayed in terms of the maximum stress and strain that occur on the outer edge of the laminate calculated on the basis of linear elasticity. Assuming homogeneity of the composite, the maximum tensile stress, σ, during three-point bending of a beam occurs on the outer edge of the laminate and is given by

$$\sigma = 6PL/4WB^2 \quad (1)$$

where P is the load at the centre point, L is the span beween the loading points, W is the sample width and B is the sample thickness. The corresponding maximum tensile strain ϵ is given by

$$\epsilon = 6B\delta/L^2 \quad (2)$$

where δ is the beam displacement at the centre point.

The falling weight clamped plate impact test used a 25 kg weight with a 10 mm radius hemispherical impactor falling at impact speeds of 3 and 6 ms^{-1} onto a $75 \times 75 \times 3.5$ mm sample clamped with a 45 mm diameter ring. The data were displayed as an impact force/time curve and the energy absorbed up to the peak value of the force calculated from this curve.

A measure of the permanent deformation of the plaque after failure was obtained by measuring the deflection normal to the plaque surface at a point 12 mm from the centre of the 45 mm diameter clamping area: damage caused by penetration of the impactor prevented measurements being made closer to the centre of the plaque.

The interlaminar shear strength (ILSS), which is a measure of the adhesion between the resin and the surface of the HMPE fibres used in these composites, was obtained from a short-beam, three-point bending test (ASTM D2344). This test is for parallel fibre composites having a loading span to sample thickness ratio of 5:1 to ensure failure in the shear mode. Leaky mould composites were prepared using an epoxy resin matrix (Ciba-Geigy HY1927) and bundles of parallel fibres to give a fibre volume fraction of 55% as described previously.[14] A $20 \times 10 \times 2$ mm composite sample was supported across a 10 mm span and tested at a displacement rate of 2 mm/min. The ILSS was calculated from the peak load:

$$\text{ILSS} = 7.357\, F / Wt \quad (3)$$

where F is the peak load in kg, W is the sample width in mm and t is the sample thickness in mm.

RESULTS

Interlaminar Shear Strength

The ILSS values obtained for the untreated and plasma-treated fibres in Table II show that in addition to the major increase in ILSS produced by plasma treatment, there is also a large difference between each fibre. Although the ILSS test requires

TABLE II
Comparison of ILSS with 0/90 three-point bend failure stress

Composite reference	Fibre	ILSS MPa	0/90 shear failure stress MPa
1	Tenfor UT†	14.5	6.8
2	Tenfor CPT	23.2	14.9
3	Spectra UT	10.0	5.2
4	Spectra CPT	17.5	10.2
5	Dyneema UT	10.6	4.8
6	Dyneema CPT	21.0	13.9

†UT, untreated; CPT, continuously plasma treated

a parallel fibre composite, a similar test can be carried out using samples cut from the 0/90 composites made for impact testing. A comparison of the ILSS and 0/90 shear failure data in Table II and Figure 1 shows that the 0/90 values are approximately 50% of the unidirectional values, although the relationship between the two tests does not appear to be linear.

High-Speed Three-Point Bend Test

For the high-speed, three-point bend test at 1 ms^{-1}, the stress-strain data are calculated from the load/displacement data using equations (1) and (2). The maximum

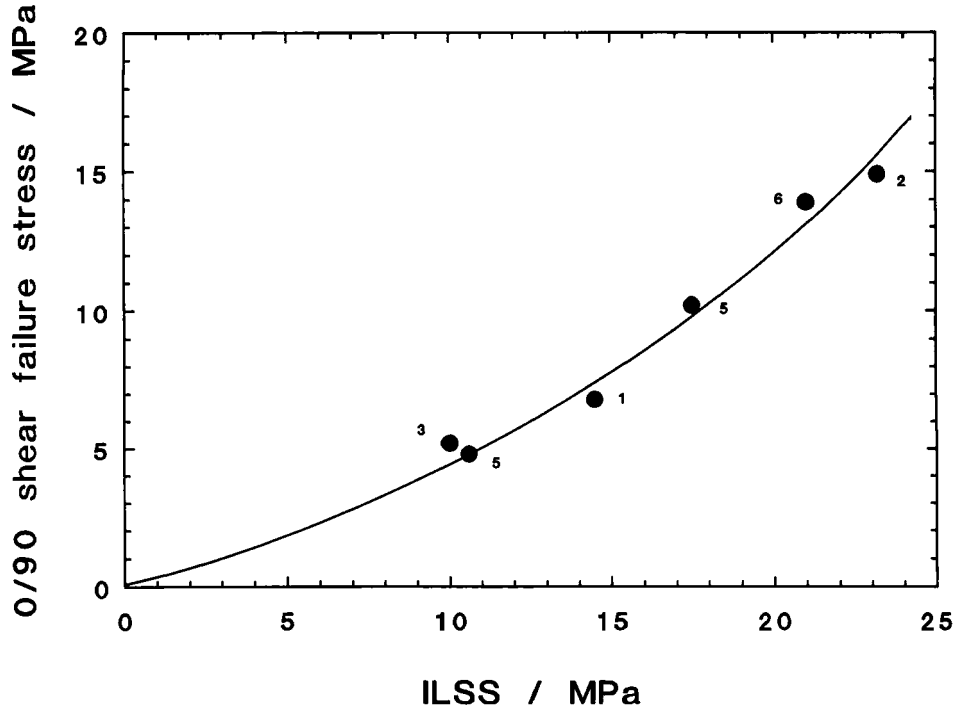

FIGURE 1 Short beam shear failure test for unidirectional and 0/90 composites.

stresses in Table III, which correspond to bending failure, are then obtained from the stress-strain data for the three fibres in Figures 2, 3 and 4. All of the impact data show periodic variations in the recorded stress values. These arise from the flexural vibrations that occur during impact but are small and of secondary importance and have, therefore, been ignored. It is seen that, in all cases, the composites containing plasma-treated fibre have a significantly higher tensile failure stress than the composites containing untreated fibre. A comparison in Figure 5 of composites made from the untreated fibres shows that the composite containing Tenfor fibre has the highest bending failure stress and Spectra has the lowest bending failure stress. For the composites made from plasma-treated fibre, Figure 6 shows that the composites containing Tenfor and Dyneema fibres now have similar failure stresses while the Spectra composite again has the lowest failure stress.

TABLE III
Three-point bend test at 1 ms^{-1}

	Stress at peak load/MPa	
Fibre	Untreated fibre	Plasma-treated fibre
Tenfor	180	220
Spectra	114	189
Dyneema	146	215

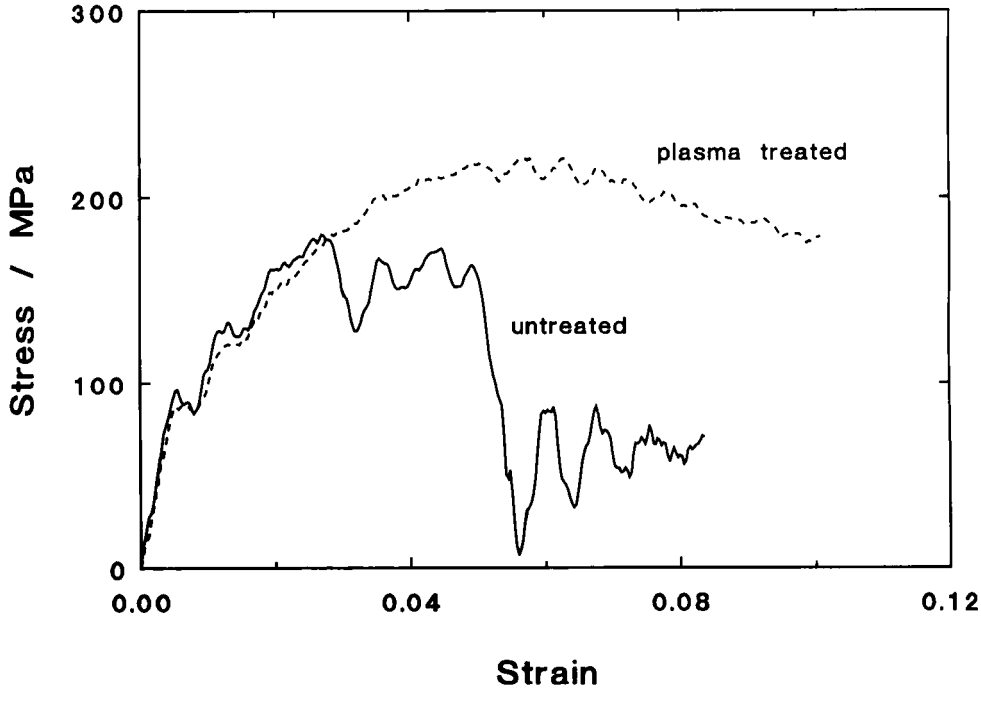

FIGURE 2 Three-point bend tests for Tenfor.

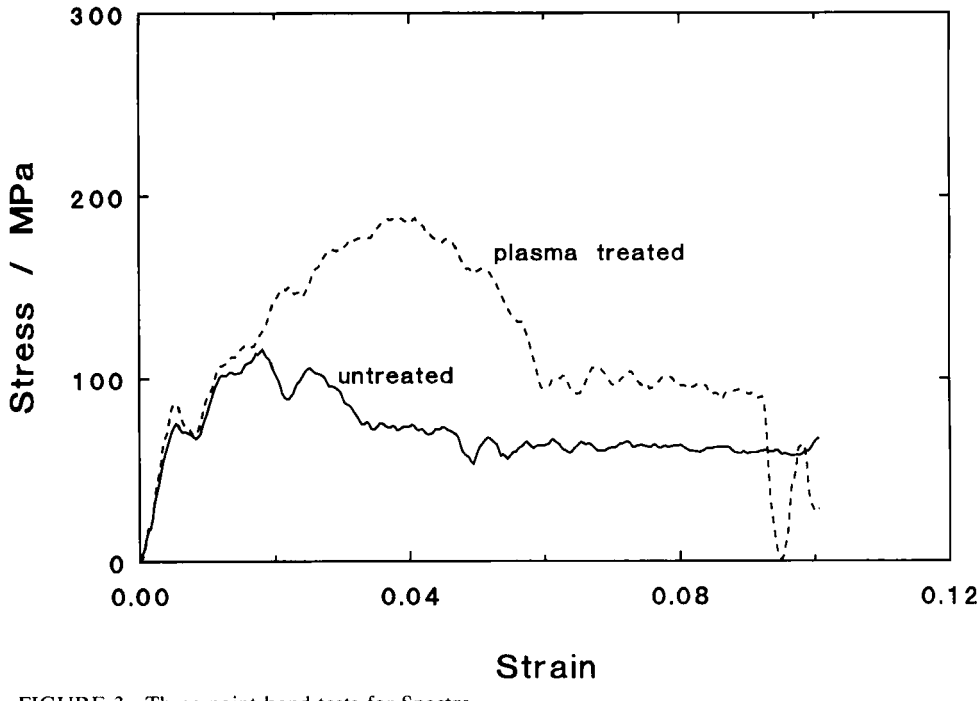

FIGURE 3 Three-point bend tests for Spectra.

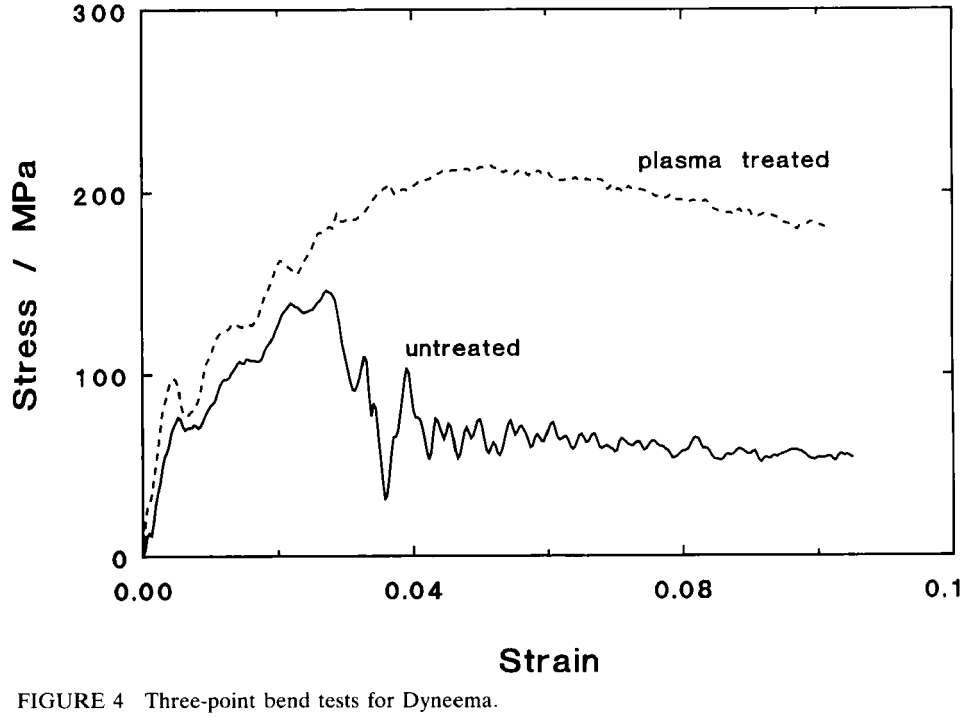

FIGURE 4 Three-point bend tests for Dyneema.

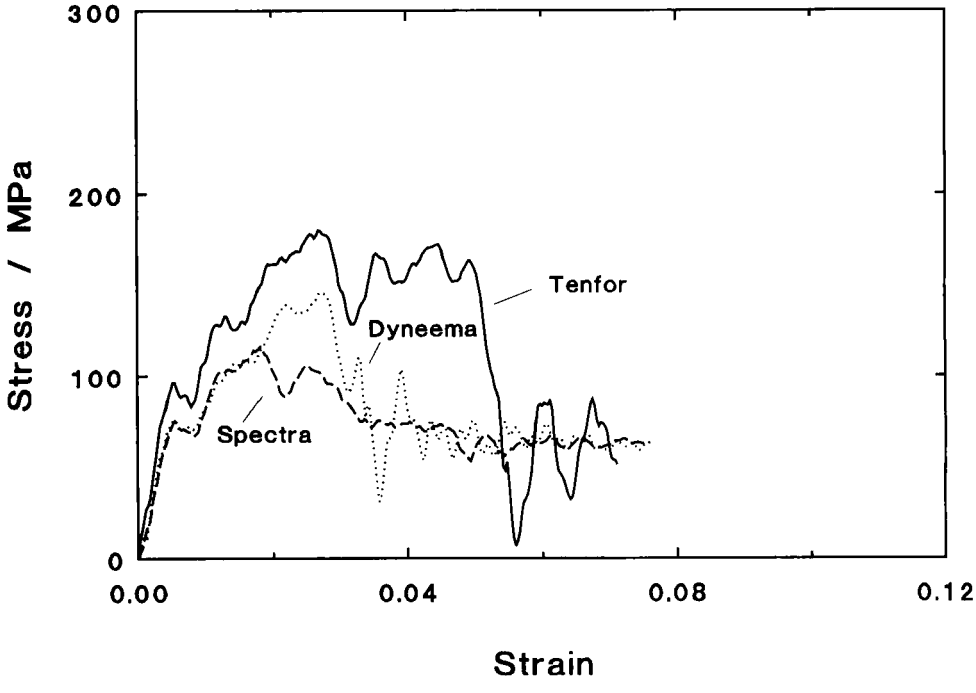

FIGURE 5 Three-point bend tests for untreated fibre.

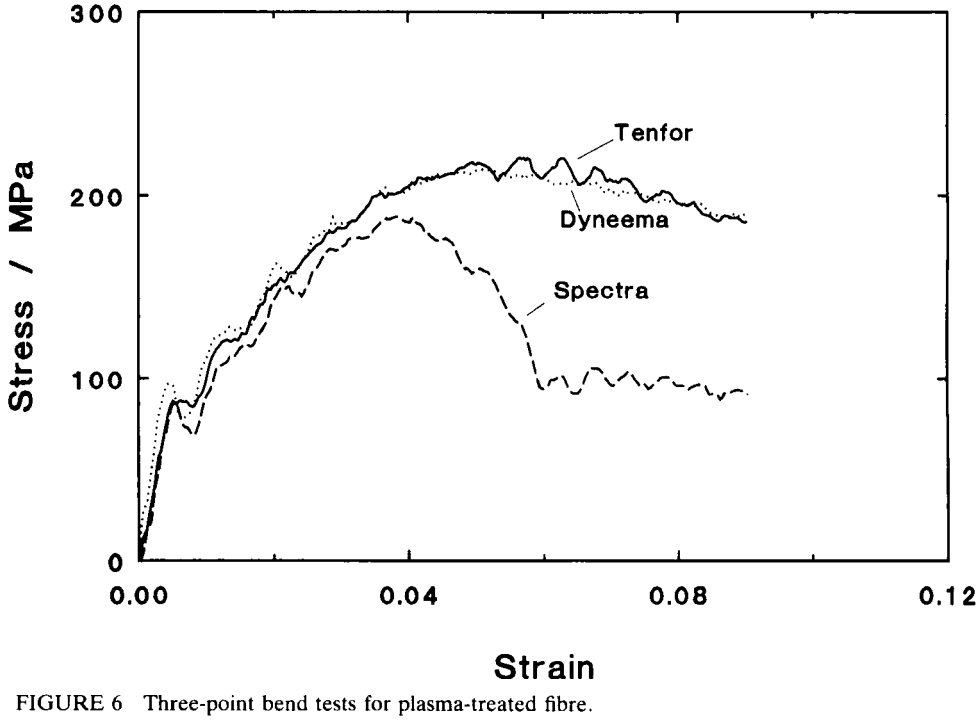

FIGURE 6 Three-point bend tests for plasma-treated fibre.

The significant increase in bending failure stress produced by plasma treatment of the fibre, and observed in Figures 2, 3 and 4, can be related to the increase in fibre/resin adhesion produced by plasma treatment. Previous work[14] has shown that the fibre/resin adhesion, as measured by ILSS using the short-beam bend test, increases significantly after plasma treating the fibre. A similar result is obtained for these composites in Table II which shows that the ILSS is increased by approximately 100% after plasma treatment.

When the maximum tensile failure stress from the three-point bend tests in Figures 2, 3 and 4 is plotted against ILSS in Figure 7, it is seen that there is a clear trend of increasing failure stress with increasing ILSS. Table IV compares the peak

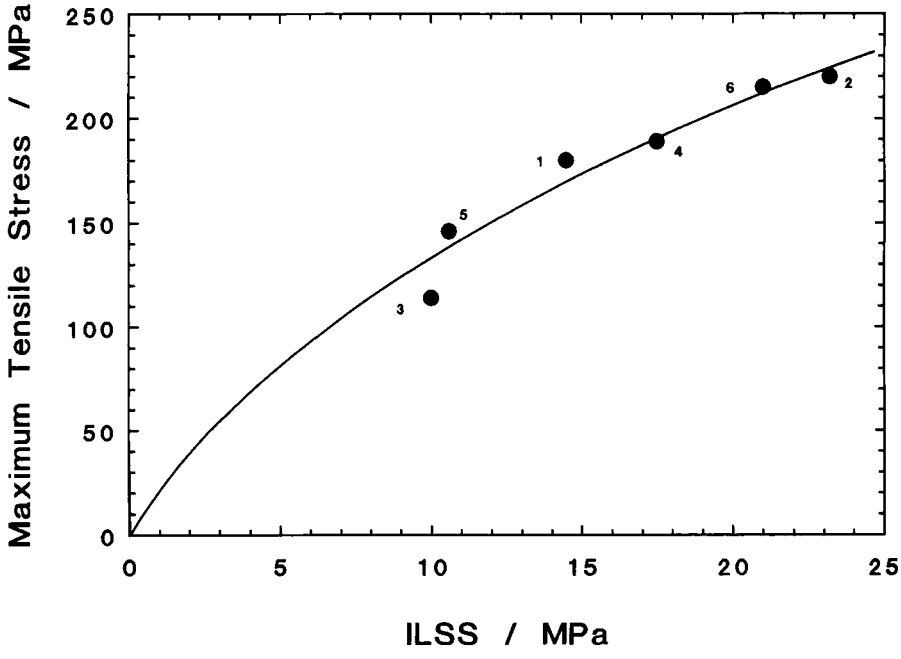

FIGURE 7 Three-point bend stress.

TABLE IV
Comparison of ILSS and three-point bend data

Fibre	ILSS MPa	Peak stress MPa	Energy to peak stress J	Strain at peak stress %	Appearance after test to a 10% strain
	Composite three-point bend test				
Spectra untreated	10.0	114	0.32	1.7	delaminated
Dyneema untreated	10.6	146	0.59	2.5	delaminated
Tenfor untreated	14.5	180	0.70	2.9	delaminated
Spectra plasma treated	17.5	189	1.09	3.9	delaminated
Dyneema plasma treated	21.0	215	1.86	5.3	no delamination
Tenfor plasma treated	23.2	220	2.19	6.3	no delamination

stress data for the high-speed, three-point bend test with the ILSS data from Table II. It is seen that ILSS, peak stress, energy to peak stress and strain at peak stress all increase in a similar manner. Inspection of the samples after testing to a constant maximum surface strain of 10% confirms that delamination, as a result of extensive shear failure, occurs in the four samples with the lowest ILSS values. The two composites having the highest ILSS do not appear to have suffered major delamination. However, since there are only minimal signs of surface fibre tensile failure, it is concluded nevertheless that the dominant cause of failure is still shear. Figure 8 also supports this view since there appears to be an approximately linear relationship between 0/90 composite strain at peak stress and ILSS.

Clamped Plate Impact Test

Table V shows the impact energy absorbed at peak load for each of the six plaques tested on the Rosand falling weight impact tester at impact speeds of 3 ms^{-1} and 6 ms^{-1}. For each of the three fibre types, it is seen that plasma treatment of the fibre produces a significant decrease in the energy absorbed at peak stress. This is in contrast to the results for the three-point bend test at 1 ms^{-1} in Table IV, where the energy absorbed at peak stress increases after plasma treatment of the fibres. Inspection of the plaques after impact testing shows that they fall into three groups:

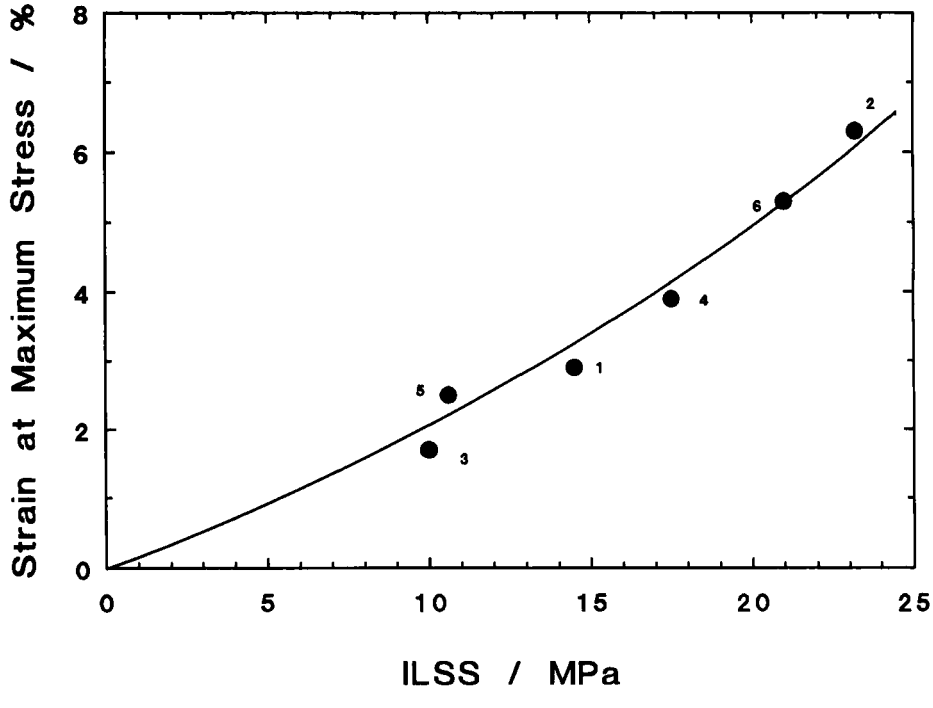

FIGURE 8 Three-point bend strain.

TABLE V
Falling weight impact—energy absorption

Composite reference	Fibre	ILSS MPa	Energy at 3 ms^{-1}	Energy at 6 ms^{-1}	Deflection at 6 ms^{-1}	Deflection × fibre strength (GPa × mm)
1	Tenfor UT	14.5	24	31	1.06	1.38
2	Tenfor CPT	23.2	12	9	0.30	0.39
3	Spectra UT	10.0	120*	128	2.85	7.41
4	Spectra CPT	17.5	101*	56	1.12	2.91
5	Dyneema UT	10.6	90*	72	2.21	5.52
6	Dyneema CPT	21.0	38	35	1.04	2.60

*Insufficient energy, sample not penetrated by impactor

Type 1, shown in Figure 9, where the falling weight has penetrated with only slight deformation within the circular clamping ring: this occurs when there is a combination of excess energy and good adhesion between fibre and resin; for example, sample 2, plasma-treated Tenfor, 75 × 75 × 3.5 mm plaque, 6 ms^{-1}.

Type 2, shown in Figure 10, where the falling weight has penetrated and there is significant deformation within the clamping ring: this occurs when there is excess

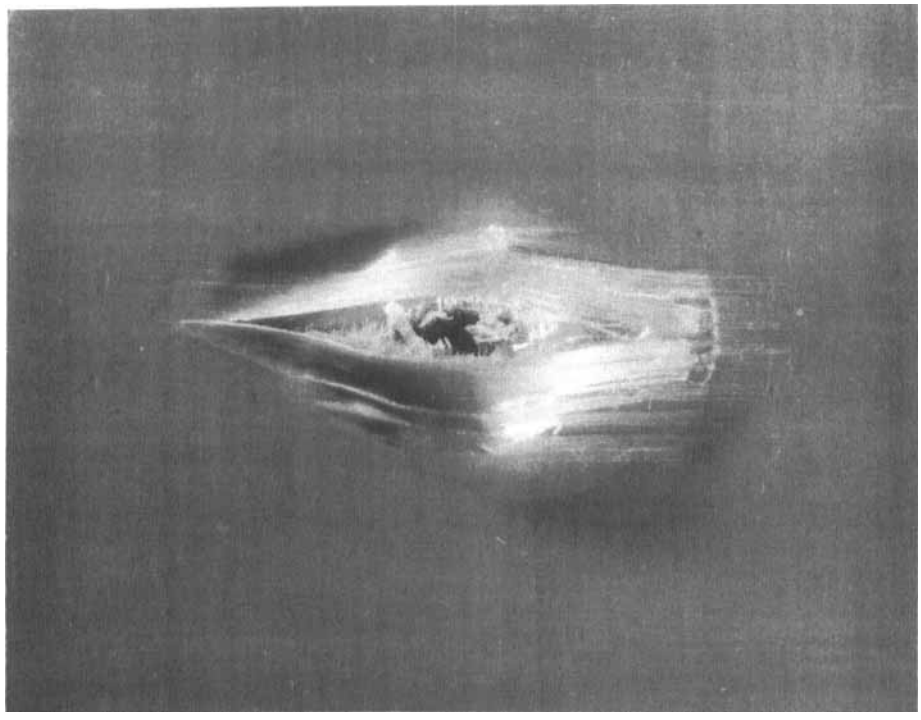

FIGURE 9 Falling weight test, penetration without delamination (*i.e.* no deformation within the clamping ring): plasma-treated Tenfor, sample 2; 75 × 75 mm plaque; 6 ms^{-1}.

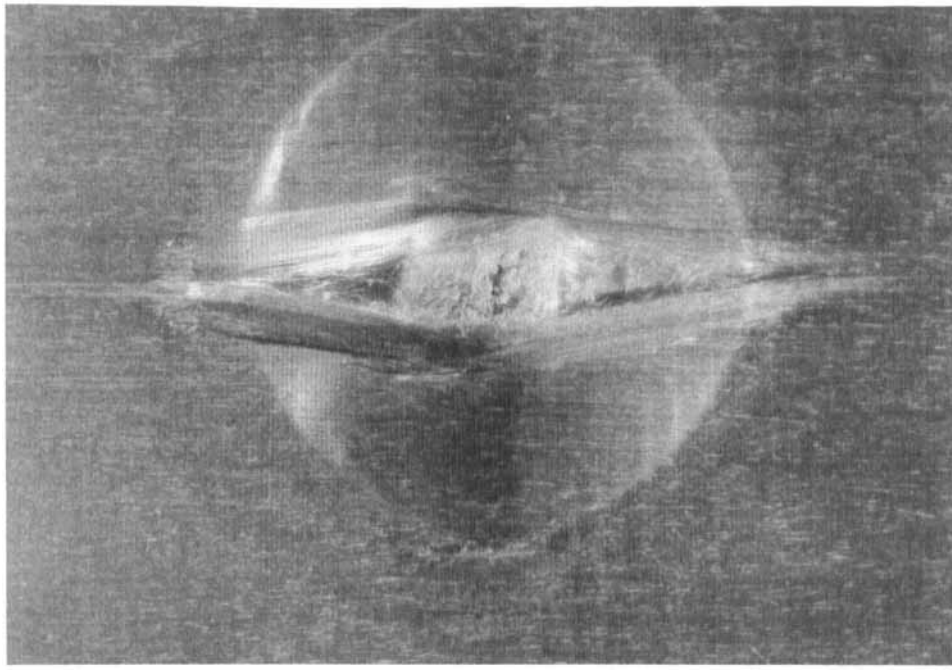

FIGURE 10 Falling weight test, penetration with delamination (*i.e.* deformation within the clamping ring): untreated Spectra, sample 3; 150 × 150 mm plaque; 6 ms^{-1}.

energy and reduced adhesion between fibre and resin; for example, sample 3, untreated Spectra, 150 × 150 × 3.5 mm plaque, 6 ms^{-1}.

Type 3, shown in Figure 11, where there is no penetration of the plaque but there is major distortion of the plaque within the clamping ring and delamination across a large area of the plaque outside the clamping ring as shown by the distortion at the edge of the composite: this occurs when there is insufficient energy to penetrate the plaque, poor adhesion between fibre and resin and the plaque area is small, allowing shear failure to extend beyond the clamping ring to the edge of the plaque; for example, sample 4, plasma-treated Spectra, 75 × 75 × 3.5 mm plaque, 3 ms^{-1}.

The first set of experiments was carried out at a speed of 3 ms^{-1}. Inspection of the failed samples showed that they could be divided into two groups: those that were penetrated by the impactor (Type 1 failure) and those that were not penetrated by the impactor (Type 3 failure). The samples that the impactor penetrated (sample 1, untreated Tenfor; sample 2, plasma-treated Tenfor; sample 6, plasma-treated Dyneema) were characterised by low absorbed energies. The samples that the impactor did not penetrate (sample 3, untreated Spectra; sample 4, plasma-treated Spectra; sample 5, untreated Dyneema) showed high energy absorption.

A second set of experiments was then carried out at an impactor speed of 6 ms^{-1}. All of the samples now showed penetration by the impactor.

The clamped plate impact energies obtained in this work cannot easily be com-

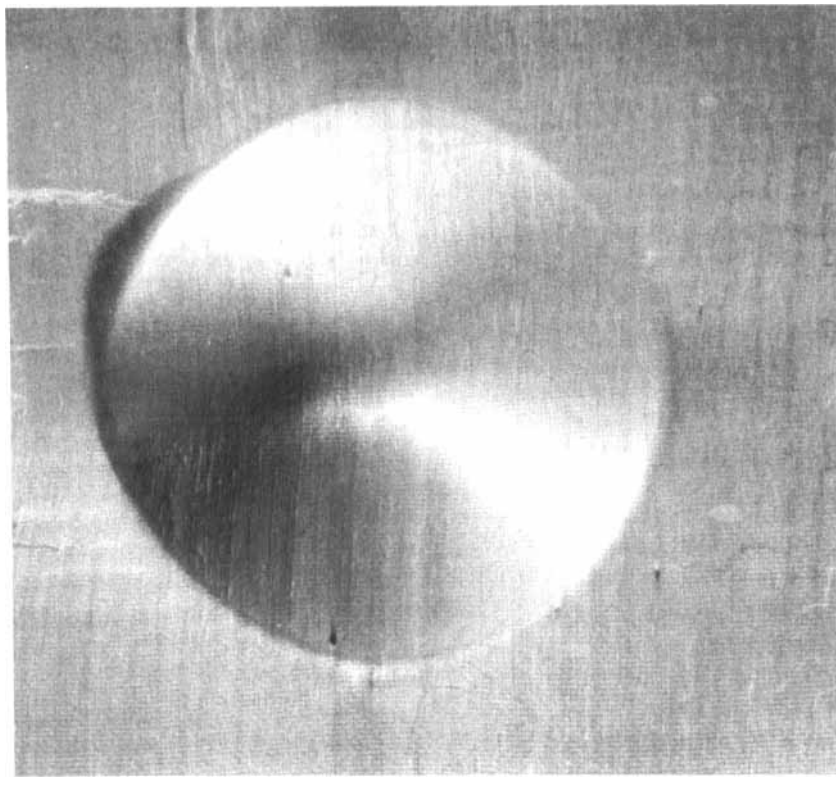

FIGURE 11 Falling weight test, delamination without penetration (*i.e.* deformation within and beyond the clamping ring): plasma-treated Spectra, sample 4; 75 × 75 mm plaque; 3 ms^{-1}.

pared with earlier work[9] since the results depend on a wide range of parameters such as fibre strength, impact velocity, clamping area and plaque size. However, the decrease in energy absorbed at peak stress following plasma treatment of the fibre, that was observed in the earlier work, is confirmed in these tests.

For the falling weight test, it is apparent that the test geometry has a major effect on the failure mode of composites that have a weak fibre/matrix interface. The samples which did not show penetration by the impactor at 3 m/s (samples 3, 4, 5) all suffered large-scale deformation both inside and outside the clamping ring to the edge of the composite. To obtain a measure of impact energy absorption that is independent of test geometry it is necessary to ensure that the sample distortion does not extend to the edges of the plate. Since the clamping ring pressure could not be increased beyond the normal operating pressure of 100 psi, the alternative of increasing the plaque size was used. The effect of increasing the size of the plaque was demonstrated by impacting 75 × 75 × 3.5 mm and 150 × 150 × 3.5 mm plaques containing untreated Spectra (sample 3) at 3 ms^{-1}. With the 75 × 75 × 3.5 mm plaque, the bulk of the distortion occurred within the ring. However, as a result of the high fibre strength, the ILSS was insufficiently high to prevent shear beyond the

clamping ring, causing distortion out to the edge of the plaque. By increasing the plaque size to $150 \times 150 \times 3.5$ mm, the delamination distortion produced on impact was restricted to the area within the clamping ring and no distortion beyond the clamping ring was observed. In both cases the energy was insufficient for penetration.

In the case of the plasma treated Tenfor, sample 2, there was no deformation beyond the clamping ring at 3 ms^{-1} with a 75×75 mm plaque and no distortion of the sample edge even when the clamping ring was removed. This is a consequence of good adhesion between the fibre and the resin (high ILSS) and relatively low fibre strength.

DISCUSSION

The two impact tests used in this work have demonstrated apparently opposing results: with the three-point bend test, the energy absorbed increases after plasma treating the fibres whereas in the falling weight test it decreases. Other workers have demonstrated an increase in epoxy resin composite flexural strength when measured at a low speed of 8×10^{-5} ms^{-1} after oxygen-plasma treatment of high-modulus polyethylene fibre, although no corresponding impact results were reported.[8] The same workers have also shown that ammonia plasma treatment of high modulus polyethylene fibres produces a composite having a higher flexural strength, measured at 8×10^{-5} ms^{-1}, and a reduced ballistic performance in terms of a V_{50} projectile test.[7] The increased flexural strength was attributed to a decrease in compressive fibre buckling and debonding resulting from a stronger fibre/matrix interfacial bond. The corresponding decrease in ballistic performance was attributed to an increase in the interfacial fibre/resin bonding which reduces the energy absorbed through fibre debonding and delamination. It will be seen that the results in this paper, where we have carried out tests at higher speed and on a range of fibres, are in broad agreement with this previous work.

In the three-point bend test there are no restrictions on shear within the sample during bending: providing the fibre has sufficient elongation at break, no filament breakage occurs at the point of maximum strain until after shear failure has occurred. The maximum shear force, which occurs at the neutral axis of the bend profile, increases progressively as the sample deflection increases until the adhesion limit is reached through failure in shear, and a peak stress is observed. Thus, as the fibre/resin adhesion (ILSS) is increased so the peak stress is increased. This explains the increase in peak stress, peak energy and peak strain in Table IV and Figures 7 and 8 resulting from an increase in fibre/resin adhesion either from plasma treatment or from different fibres. The three-point bend failure is, therefore, relatively insensitive to fibre strength.

In the falling weight test, the test sample is held in a clamping ring which, together with the test sample geometry, restricts the deformation produced by the impactor. As a result, the tensile strength of the composite fibres will influence the failure energy, and the energy absorbed by the plaque will be dependent on 1) the fibre/resin adhesion, 2) the energy absorbed by the fibres and 3) the test geom-

etry. It appears that impacted plaque failure occurs in two stages: deformation of the area within the clamping ring followed by penetration of the impactor. Following impact, the plaque deforms in conical form within the clamping area until the peak stress at the plaque centre approaches the fibre failure stress. All of the fibres within, and possibly beyond, the clamped area will be strained by an amount dependent on the extent of shear failure, and will provide the major source of energy absorption. At this point, the impactor penetrates the weakened central area of the plaque.

With good adhesion between the fibre and the resin, the plaque deforms to failure in a normal bending mode with 1) a central neutral axis and 2) a peak bending stress at the central point of the convex surface. For small deformations, the composite strain will be proportional to the amount of deformation of the plaque.

Assuming that, in all cases of plaque failure by penetration of the impactor, the fibre strain within the deformation area approaches the fibre breaking strain, then the energy absorbed by the fibre will be approximately proportional to the product of the plaque deformation and the fibre strength. The relatively small contribution of the 46% volume of low modulus resin can be ignored.

It is suggested that the amount of shear that occurs during the plaque deformation is controlled by the fibre/resin adhesion: measurements of the permanent deformation of the plaque after tests at 6 ms^{-1} confirm this, Figure 12 showing that the plaque deformation at failure is dependent on ILSS. As the shear increases as a

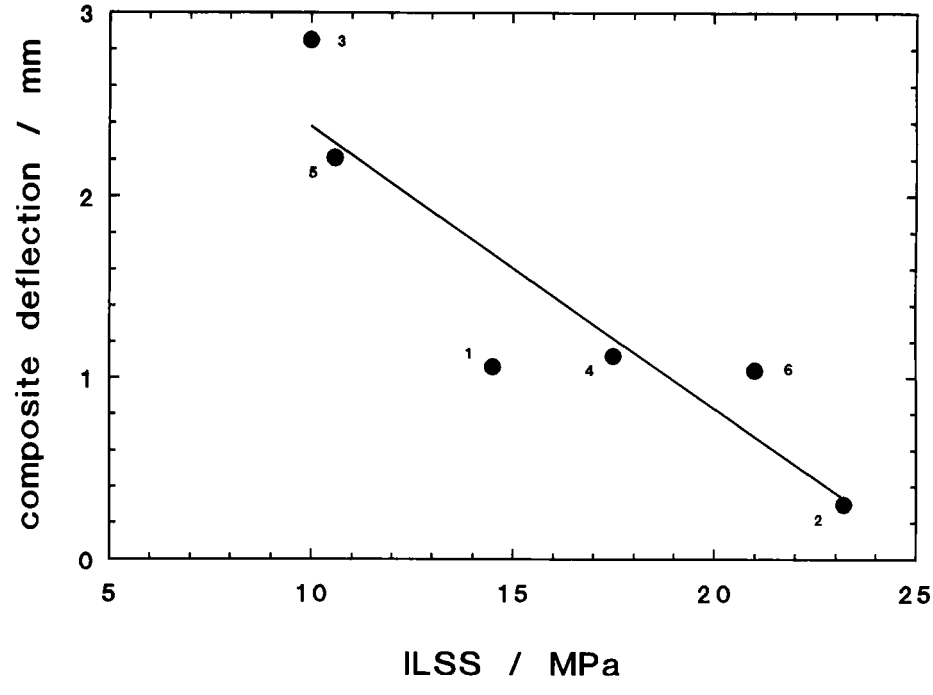

FIGURE 12 Falling weight test: plaque deformation at 6 ms^{-1}.

result of reducing the ILSS, the stress in the fibres in the shear zone will relax and the deformation at which the fibres reach their breaking strain will, therefore, increase.

The energy absorbed after impact will, therefore, relate to the energy required to strain the fibres in the shear zone which will be proportional to the product of the plaque deformation and the fibre strength. This is confirmed in Figure 13 which shows that a measure of energy absorption, obtained from the product of the fibre strength and the plaque deflection, relates directly to energy absorption obtained from the falling weight impact results. Since the regression line fitted to the data in Figure 13 extrapolates approximately to zero energy at zero deformation, it appears that the ILSS and fibre strength are the major contributors to impact energy absorption for a particular test geometry.

These results suggest that it should be possible for the plaque energy absorption to be calculated from a knowledge of the fibre-to-resin adhesion (ILSS) and the fibre strength. The results also explain why, in contrast to the three-point bend test, the energy absorbed in the falling weight test decreases when the ILSS is increased by plasma treatment. With the three-point bend test, the peak energy occurs at the onset of shear. With the falling weight test, the plaque is effectively restrained by both the clamping ring and the sample geometry with the result that fibre strain increases significantly after shear failure occurs.

It has been shown that composite failure can involve fibre/resin shear failure and

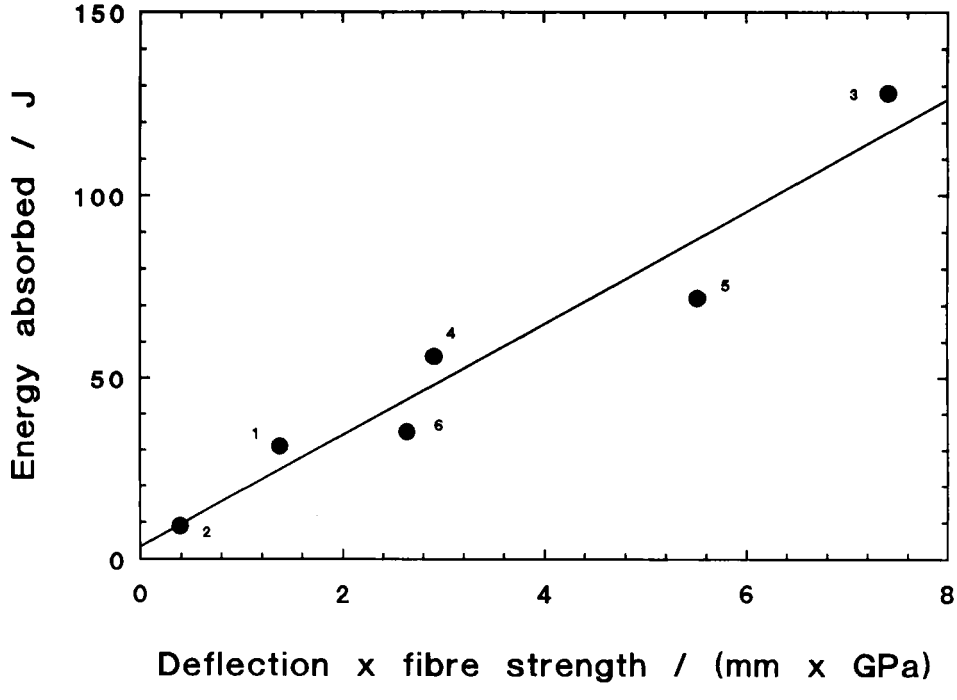

FIGURE 13 Falling weight test; energy absorption at 6 ms^{-1}.

fibre tensile failure. The three-point bend test which mainly involves shear failure and the falling weight test which involves both shear and tensile failure are, therefore, seen as complementary tests and are both valid for assessing impact behaviour.

CONCLUSIONS

It is shown that a high-speed, three-point bend test can be used to assess the impact performance of 0/90 HMPE melt- and gel-spun fibre/epoxy resin composites. Plasma treatment of the fibres increases the failure stress of each composite and a linear relationship between the peak stress and the fibre/resin adhesion as measured by the interlaminar shear strength, independently of fibre strength, is demonstrated. It is thought that this test represents a useful measure of assessing composite damage tolerance.

Impact testing of composite plaques using a falling weight with sufficient energy to ensure penetration at approximately constant velocity does not necessarily produce a simple relationship between fibre/resin adhesion and absorbed energy because of the dependence on a wide range of parameters such as fibre strength and testing geometry. For this test, several additional factors such as clamping method and fibre strength also have to be considered when assessing plaque damage tolerance. However, it appears that, in general terms, the falling weight impact energy increases with increasing fibre strength and decreasing interlaminar shear strength.

References

1. I. M. Ward and N. H. Ladizesky, *Pure Appl. Chem.*, **57**, 1641–1649 (1985).
2. N. H. Ladizesky and I. M. Ward, *Comp. Sci. Technol*, **26**, 199–224 (1986).
3. B. Harris, in *High modulus polymers and composites*, C. L. Choy, Ed. (Chinese University Press, Hong Kong, 1984).
4. A. E. Johnson, D. R. Moore, R. C. Prediger, P. E. Reed and S. Turner, *J. Mater. Sci.*, **21**, 3153–3161, (1986).
5. A. A. J. M. Peijs, R. W. Venderbosch and P. J. Lemstra, *Composites*, **21**, 522–530, (1990).
6. J. R. Brown, P. J. C. Chappell and Z. Mathys, *J. Mater. Sci.*, **26**, 4172–4178, (1991).
7. J. R. Brown, P. J. C. Chappell and Z. Mathys, *J. Mater. Sci.*, **27**, 3167–3172, (1992).
8. J. R. Brown, P. J. C. Chappell and Z. Mathys, *J. Mater. Sci.*, **27**, 6475–6480, (1992).
9. B. Tissington, G. Pollard and I. M. Ward, *Comp. Sci. Technol.*, **44**, 197–208 (1992).
10. B. Tissington, G. Pollard and I. M. Ward, *J. Mater. Sci.*, **26**, 82–92 (1991).
11. B. Tissington, G. Pollard and I. M. Ward, *Comp. Sci. Technol.*, **44**, 185–195 (1992).
12. D. W. Woods and I. M. Ward, *Surf. Interface Anal.*, **20**, 385–392 (1993).
13. N. H. Ladizesky, I. M. Ward and L. N. Phillips, U.S. Pat. 4410586 (1983), European Patent 82301689.4 (1982).
14. N. H. Ladizesky and I. M. Ward, *Comp. Sci. Technol.*, **26**, 129–164 (1986).